Galactic Cosmic Ray Radiation Hazard in the Unusual Extended Solar Minimum between Solar Cycle 23 and 24

N. A. Schwadron, A. J. Boyd, K. Kozarev

Boston University, Boston, Mass, USA

M. Golightly, H. Spence

University of New Hampshire, Durham New Hampshire, USA

L. W. Townsend

University of Tennessee, Knoxville, TN, USA

M. Owens

Space Environment Physics Group, Department of Meteorology, University of Reading, UK

Abstract. Galactic Cosmic Rays (GCRs) are extremely difficult to shield against and pose one of most severe long-term hazards for human exploration of space. The recent solar minimum between solar cycle 23 and 24 shows a prolonged period of reduced solar activity and low interplanetary magnetic field strengths. As a result, the modulation of GCRs is very weak, and the fluxes of GCRs are near their highest levels in the last 25 years in the Fall of 2009. Here, we explore the dose-rates of GCRs in the current prolonged solar minimum and make predictions for the Lunar Reconnaissance Orbiter (LRO) Cosmic Ray Telescope for the Effects of Radiation (CRaTER), which is now measuring GCRs in the lunar environment. Our results confirm the weak modulation of GCRs leading to the largest dose rates seen in the last 25 years over a prolonged period of little solar activity.

Background – Galactic Cosmic Rays and Human Health

In balloon flights in 1912-1913, Hess first measured a form of radiation that intensified with altitude [*Hess*, 1912; 1913]. Millikan realized that this radiation couldn't come from the Sun since its intensity didn't vary from day to night, and thus called it "Cosmic Ray" radiation [*Millikan and Bowen*, 1926]. The majority of this radiation is from Galactic Comic Rays (GCRs), which are accelerated outside our Solar System, most likely by the strong shocks that result from supernova explosions in our galaxy. GCRs have enormous energies (100 MeV -10 GeV) and near-light speeds. They continually bombard Earth's atmosphere, producing secondary particles and radiation through cascading high-energy collisions.

Because most GCR radiation that penetrates into the near-Earth space environment is shielded by Earth's magnetic field, it does not pose a common health hazard. However, during space travel, GCRs are difficult to shield [*Wilson et al.,* 1991; *Cucinotta et al.,* 2001] since they produce secondary radiation in shielding and other material that is even more hazardous than the GCRs themselves. On long duration missions, GCR radiation is the primary health hazard to astronauts [*NAS*, 1973, 1997; *Cucinotta et al.,* 2001a].

In the outer heliosphere, beyond ~100 AU, the slowing of solar wind is thought to form a large magnetic barrier that shields out >90% of the GCR radiation present in interstellar space [Florinski et al., 2003a] at energies below ~100 MeV. Because this reduction is so large, even a very small change in the shielding efficiency can have a large impact on the radiation environment in the solar system. However, because these regions have never been directly sampled or observed, there is great uncertainty about the physics of outer heliospheric shielding and its sensitivity to changes in the solar wind output and the local interstellar medium. A small

fraction of GCRs penetrate into the heliosphere and propagate toward the Sun and planets. These residual GCRs are modulated by the solar wind's magnetic field in the inner heliosphere.

Forbush (1954) discovered the ~11-year modulation of GCRs, which is explained by the transport of GCRs through heliopheric magnetic fields (Parker, 1965; Gleeson and Axford, 1968; Urch and Gleeson, 1972). During periods of high solar activity (solar maximum), which occur each ~11 years, the heliospheric magnetic field magnitudes increase due to a much larger rate of Coronal Mass Ejections (CMEs) from the Sun. As a result, the solar wind's intense solar maximum magnetic field is more effective at sweeping GCRs out of the inner heliosphere, which causes a strong reduction of the GCR flux. A 22-year cycle is also evident: GCR flux maxima are typically sharply peaked for even numbered solar minima (when the large scale solar magnetic field is inward in the North; $A < 0$), whereas odd numbered solar minima (when the solar magnetic field is outward in the North; $A > 0$) show more broadly peaked GCR flux maxima. Over the 22-year solar magnetic cycle, known as the Hale cycle, the large-scale solar magnetic field reverses its polarity over the first solar activity cycle (~11 years) and then returns to its original polarity in the next solar activity cycle. Most of the actual magnetic reversal happens over a 2-4 year period centered on solar maximum and is thought to be forced by the release of CMEs (Owens et al., 2007; Schwadron et al., 2008). The solar magnetic reversal has a strong effect on the entry of GCRs into the heliosphere. Positively charged cosmic rays drift in from the heliospheric polar regions when the Sun's north polar field is directed outward ($A > 0$). In contrast, when the Sun's north polar field is directed inward ($A < 0$), positively charged cosmic rays drift inward along the heliospheric current sheet where they are scattered by irregularities in the current sheet, by Coronal Mass Ejections and other large-scale interaction regions.

72 Conversely, negatively charged cosmic rays (electrons) drift inward from directions
73 opposite to the positively charged cosmic rays. Potgieter and le Roux (1992) and Ferreira
74 and Potgieter (2004) approximately reproduce the ~22-year cycle in the GCR fluxes
75 using a time-dependent modulation model, which includes gradient, curvature, and
76 current-sheet drift effects (Jokipii, Levy, and Hubbard, 1977) and diffusion parallel and
77 perpendicular to the magnetic field.

78 Large changes in the Local Interstellar Medium (LISM) have dramatic effects on the
79 heliosphere and the radiation environment of the solar system. For example, a typical
80 enhancement in the density of the local interstellar medium by a factor of 10 causes the entire
81 heliosphere to shrink to about a quarter of its current size [*Zank and Frisch*, 1999], and increases
82 the fluxes of GCRs at Earth by a factor of 2-6 [*Scherer et al.,* 2002]. Such large changes in the
83 LISM have certainly occurred in the past and will occur again in the future [*Zank and Frisch*,
84 1999].

85 We do not currently have the observational knowledge required to understand how the
86 local interstellar medium interacts with the heliosphere; continued observations such as those
87 provided by the Interstellar Boundary Explorer mission (IBEX; *McComas et al.,* 2009) and the
88 Voyager satellites [e.g., *Stone et al.,* 2005; *Richardson et al.,* 2008] are important for better
89 understanding the radiation environment that must be traversed by astronauts for long missions to
90 distant destinations such as Mars.

91 On Earth, radioisotope ^{10}Be provides a recent record of cosmic ray fluxes. The isotope is
92 produced in Earth's upper atmosphere by spallation reactions of cosmic rays (CR) protons with
93 energies higher than about 100 MeV and secondary neutrons with atmospheric nitrogen and
94 oxygen [*Masarik and Beer*, 1999]. ^{10}Be records in Antarctic ice show two prominent peaks

35,000 and 60,000 years ago, when the radioisotopoe production rate was about twice the current value for about 1500 and 2000 years, respectively [*Raisbeck et al.,* 1987]. The 35,0000 year peak is also present in marine sediment records [*Cini Castagnoli et al.,* 1995; *McHargue et al.,* 1995]. The fact that the ^{10}Be radioisotope changes significantly with time shows that significant changes in cosmic ray fluxes have occurred in the past. But the cause for these changes remains controversial. The most accepted explanation is that the peaks are caused by geomagnetic magnetic field excursions, which is supported by the observed correlation between geomagnetic field strength and ^{10}Be levels in marine sediment records [*McHargue et al.,* 2000; *Wagner et al.,* 2000]. However, this explanation would suggest that the ^{10}Be enhancements should be uniform over the globe, which contradicts the large variations observed at high latitudes where geomagnetic effects are small. Further, *Cini Castagnoli et al.* [1998] found that the ^{10}Be level starts to increase some 2000 years before the drop in Earth's magnetic field, as reflected by the magnetization measured in the same core sample. Thus, many of the long-term changes in the cosmic ray fluxes incident on Earth may be due to effects external to the Earth; either due to changes in the shielding of the inner heliosheath or due to changes in the incident fluxes of GCRs from outside the heliosphere.

Could the GCR fluxes in the heliosphere change rapidly in the future due to rapidly changing conditions in the LISM? For the period from 1700 AD to present-day, the ^{10}Be record from ice cores can be compared with sunspot data [*Beer et al.,* 1990]. The result is a remarkably steady anti-correlation, which demonstrates how changes in the solar wind's magnetic field over the solar cycle affect GCRs in the inner solar system. As described above, higher solar activity (when sunspot numbers are large) is correlated with increased interplanetary magnetic field strength, which, in turn, reduces the number of GCRs entering the inner heliosphere. A further

118 implication of the strong and remarkably steady anti-correlation between sunspot number and
119 GCR flux is that, over the last 300 years, the incident flux of GCRs on the heliosphere, and the
120 shielding of GCRs in the inner heliosheath have been relatively constant.

121 The primary question taken up in this paper is the dose-rates induced by GCRs. The
122 GCR environmental model of *Badhwar and O'Neill* [Badwhar and O'Neill, 1991; 1992;
123 1993; 1994; 1996] is used to model the species-dependent GCR flux over time. The
124 *Badhwar-O'Neill* model is based on the fitting of measured differential energy spectra to
125 stationary solutions of the Fokker-Planck equation parameterized by an assumed form for
126 the diffusion coefficient that varies as a function of the interplanetary modulation
127 potential (measured in MV). The High-charge(Z)-and Energy (HZE) TRaNsport code
128 (HZETRN) is solved using a one-dimensional, analytical formulation of the Boltzmann
129 transport equation to describe the transport of GCRs through shielding and tissue. The
130 effect of the long-range Coulomb force and electron interaction is treated as a continuous
131 slowing-down process. Atomic (electronic) stopping power coefficients with energies
132 above a few MeV/nucleon are calculated using Bethe's theory including Bragg's rule,
133 Ziegler's shell corrections, and effective charge. Nuclear reaction cross-sections are
134 obtained from curve fits to quantum scattering calculations and total cross sections are
135 obtained with a Ramsauer formalism. Nuclear fragmentation cross sections are calculated
136 with a semiempirical abrasion-ablation fragmentation model, NUCFRG2, also developed
137 at NASA Langley. The code transports heavy charged particles (Z =1 through 26) in the
138 incident GCR spectrum, and all of their reaction products, including secondary neutrons,
139 through as many as 5 layers of shield materials and water, which is used as a surrogate
140 for human tissue. The output from the code includes particle fluxes or fluences for all

heavy charged particles and neutrons, absorbed dose, dose equivalents, and linear energy transfer (LET) spectra in water for any desired location in any of the shield materials.

A 3-layer version of HZETRN 2005 has been configured for the Earth-Moon-Mars Radiation Environment Module (EMMREM) to calculate GCR dose and dose equivalent [*Townsend et al.,* 2009a]. The code has been used to develop a look-up table of daily effective dose, organ doses and dose equivalents behind varying thicknesses of aluminum shielding. GCR flux input into the calculations is taken from the *Badhwar-O'Neill* GCR model using modulation potentials ranging from the most highly probable solar minimum (400 MV) to solar maximum conditions (1800 MV) in the solar cycle. This model is the standard one used for space operations at the Space Radiation Analysis Group (SRAG) at NASA Johnson Space Center. A look-up table is used because the large spread in interplanetary magnetic field conditions, large numbers of GCR ion species and their many reaction product secondary particles must be transported through as much as 500 g/cm^2 of shield materials. Calculations of such complex spectra at such depths take approximately half a day for each possible spectrum and cannot be carried out in near real time simulations. Since GCR intensities change very little from day to day, daily dose and dose equivalent estimates are sufficient.

The changes in GCRs in an extended Solar Minimum (Cycle 23 to 24)

The solar minimum between Cycle 23 and 24 is proving to be extremely interesting. The Sun is remarkably quiet. Recent observations have found that the strength of the interplanetary magnetic field [*Owens et al.,* 2008] has been falling off to new low levels observed during the space-age. Figure 1 shows the evolution of the interplanetary magnetic field strength. The

precipitous recent drop in the observed magnetic field strength is seen at multiple spacecraft and appears to be related to a global reduction in the magnetic flux of the heliosphere.

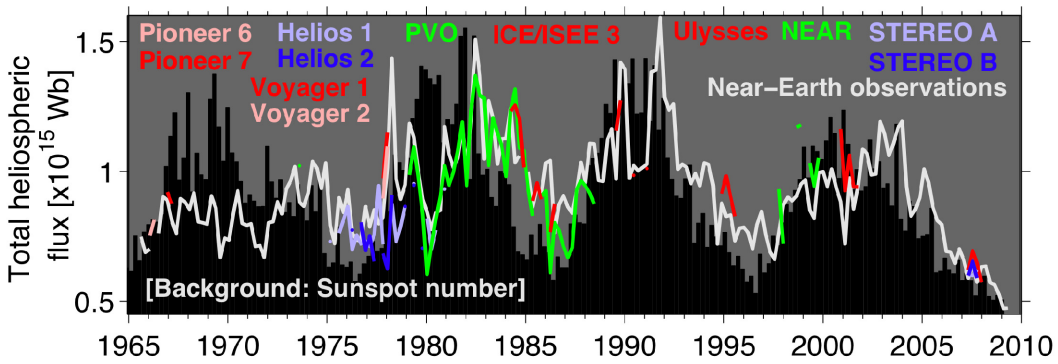

Fig. 1. Total heliospheric magnetic flux estimated from in situ spacecraft observations over four complete solar cycles. Sunspot number is shown as the black background. There is an approximate doubling of heliospheric flux from solar minimum to maximum [which may be the result of closed flux added to the heliosphere by Coronal Mass Ejections]. The current minimum is exhibiting the lowest flux yet observed. Figure adapted from Owens et al., 2008.

We show in Figure 2 the modulation potential derived from neutron fluxes at Earth and cosmic rays observed at ACE [*O'Neil*, 2006]. The modulation potential is derived from the modulation parameter,

$$\phi(r) = \int_{r}^{R_b} \frac{V(x)}{3\kappa_1(x)} dx \qquad (1)$$

where the modulation potential is $\Phi = |Z\,e|\varphi(r)$. The integral in (1) extends from the inner boundary at radius r to the outer modulation boundary R_b, the solar wind speed is $V(x)$ and $\kappa_1(x)$ is related to the radial diffusion coefficient, κ. In particular, the form for κ is based on a fit to the observed spectrum over time and species [*O'Neil and*

Badhwar, 2006]: $\kappa = \kappa_1(r)\, P\, \beta$ where P is the rigidity in GV, β is the particle speed over the speed of light, $\kappa_1(r) \propto 1 + (r/r_0)^2$ and $r_0 = 4$ AU. In the *Badhwar-O'Neill* model, reductions in the modulation potential are caused by enhanced diffusion, allowing greater access and therefore higher fluxes of GCRs in the inner heliosphere.

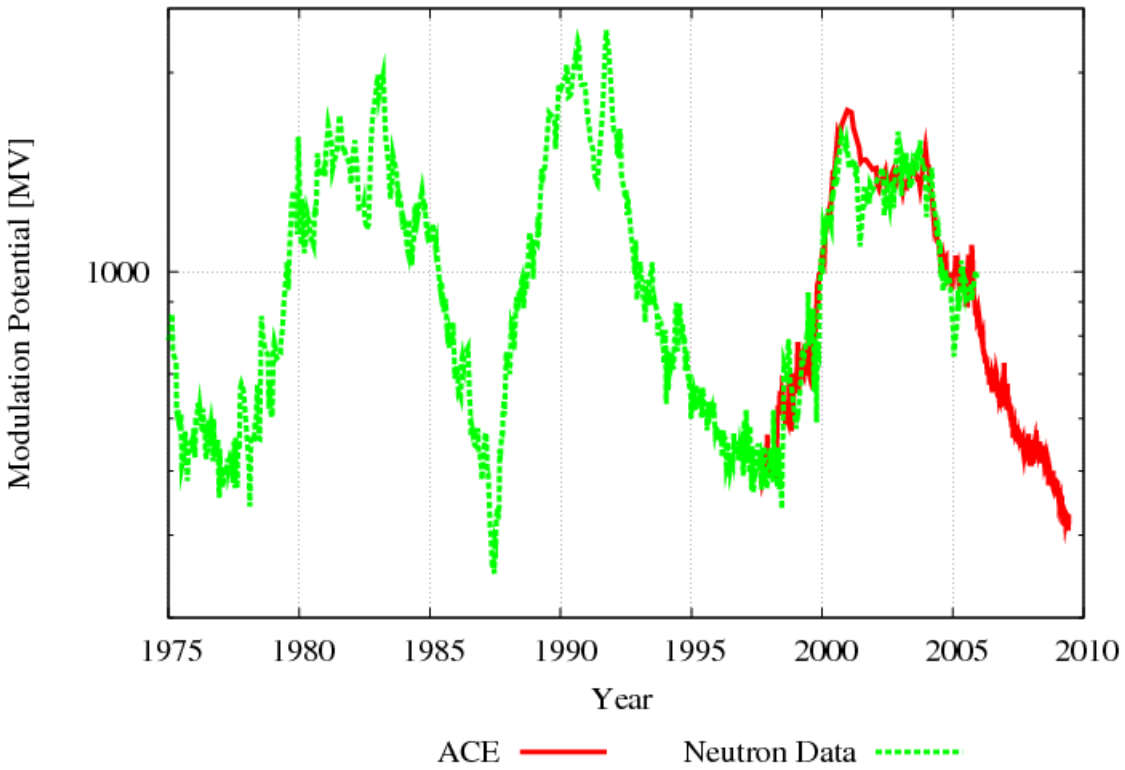

Fig. 2: The modulation parameter based on observations of neutrons using Climax data and on the Advanced Composition Explorer (ACE) Cosmic Ray Isotope Spectrometer (CRIS) measurements [O'Neil, 2006].

Saganti et al. (2006) show a comparison between the *Badwhar-O'Neill* model with HZETRN and MARIE Mars observations. They find 21.2 mrad/day predicted by the model versus 21.4 mrad/day measured observed by MARIE. Thus, the combination of HZETRN and the *Badwhar-O'Neill* model provides an accurate determination of dose

and dose-rate. The predictions that follow will eventually be compared to measurements from the Lunar Reconnaissance Orbiter (LRO) Cosmic Ray Telescope for the Effects of Radiation (CRaTER).

Figure 3 shows the dose rates to the Skin, Central Nervous System (CNS), Blood Forming Organs (BFO) and the Lens using the combination of HZETRN and the *Badwhar-O'Neill* model for a variety of different shielding levels from 0.3 g/cm^2 to 100 g/cm^2. These doses are calculated in free space where surfaces are exposed over 4π ster-radians.

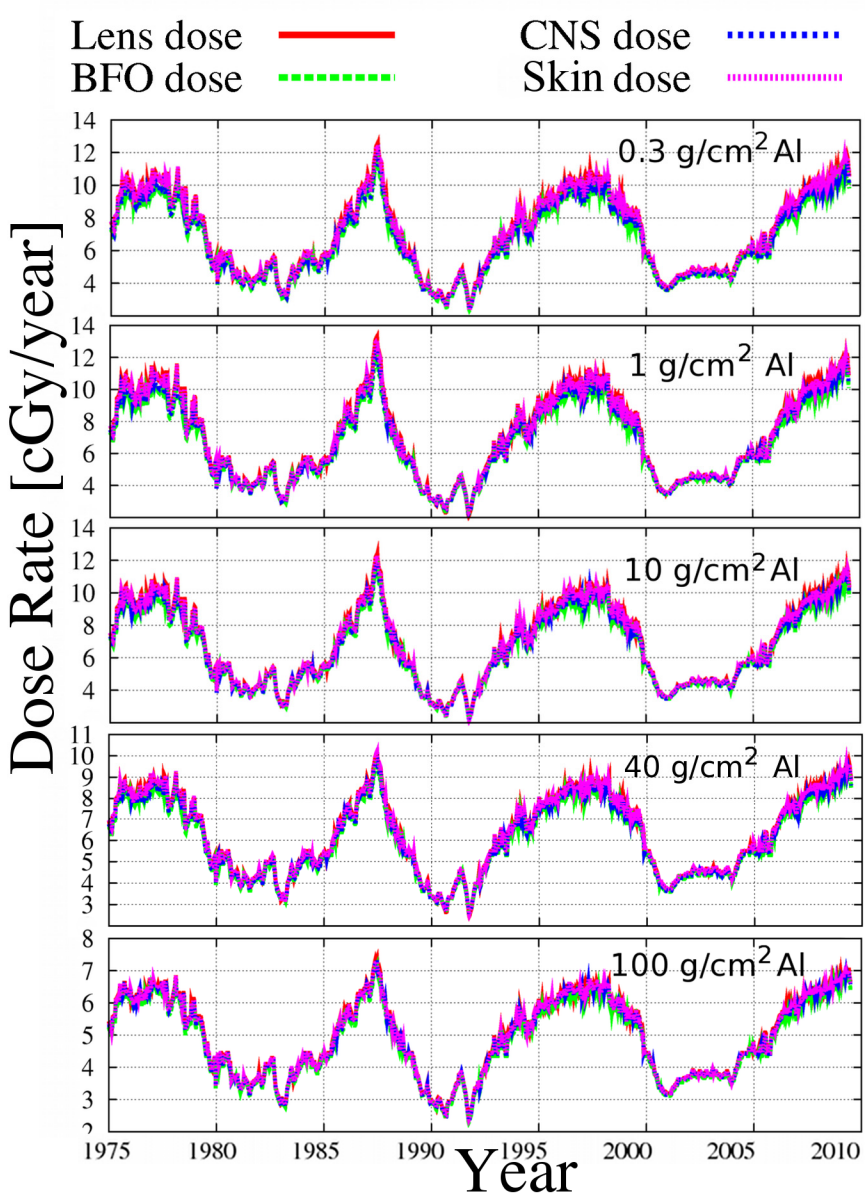

205

206 *Fig. 3*: *Dose rates from GCRs in free space behind different levels of Al shielding ranging*

207 *from 0.3 to 100 g/cm*^{2}. *These predictions have been made using a 3-layer version of*

208 *HZETRN 2005, which has been configured to calculate GCR dose and dose equivalents*

209 *[Townsend et al., 2009a] based on GCR fluxes from Badhwar-O'Neill GCR model. We*

210 *have calculated doses to the Lens, Central Nervous System, Blood Forming Organs, and*

211 *the Skin.*

212

213 Figure 4 shows the results for the dose-equivalent rates, which take into account
214 quality factors and relative biological effectiveness for the different species composing
215 galactic cosmic rays. The dose-equivalent rates are substantial. For example, behind 0.3
216 g/cm^2 Al we find dose rates between 25 and 35 cSv/year, which approach dose limits of
217 52 cSv (for a 25 year old male), 37 cSv (for a 25 year old female), 72 cSv (for a 35 year
218 old male), and 55 cSv (35 year-old female) for 1-year missions and average life-loss for
219 an exposure-induced death for radiation carcinogenesis (Table 3, NASA-STD-3001,
220 2007).

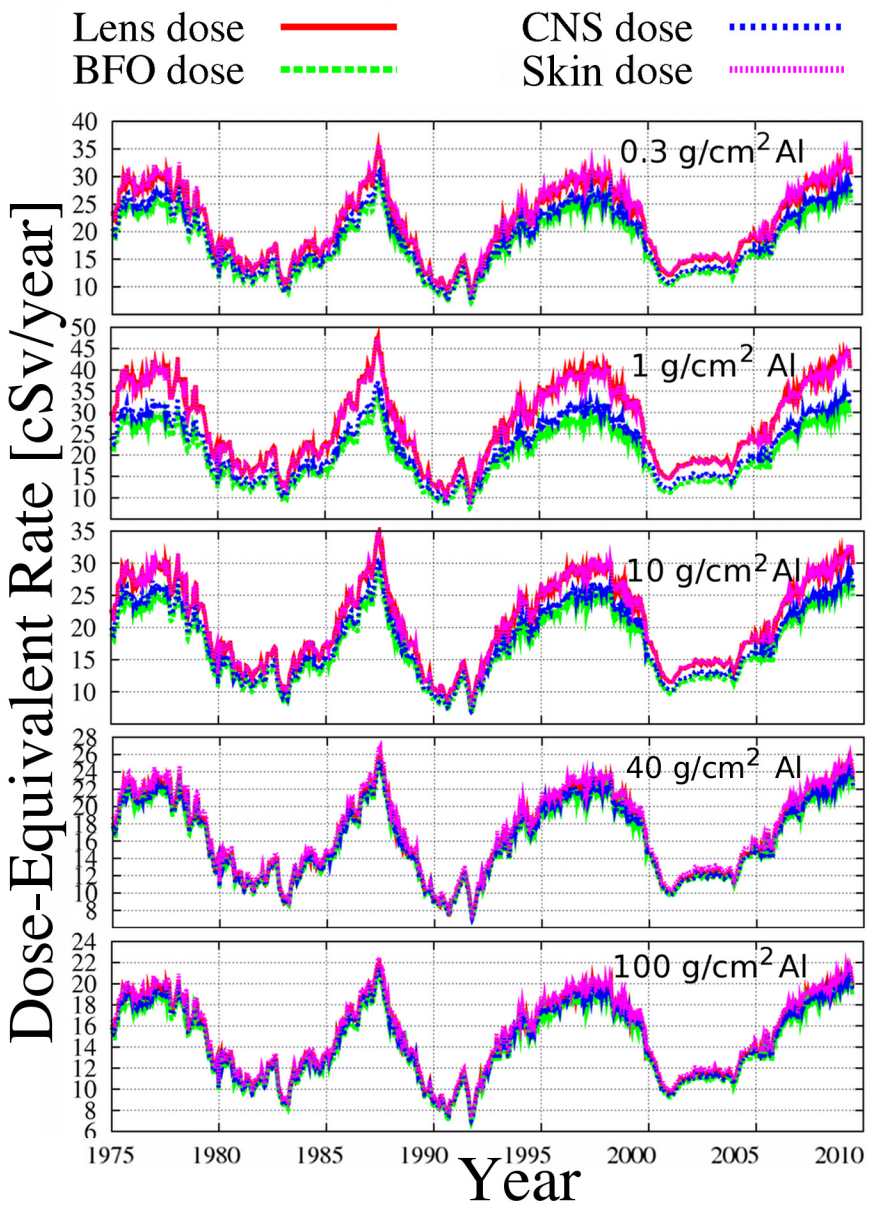

Fig. 4: *Dose equivalent rates from GCRs in free space behind different levels of Al shielding ranging from 0.3 to 100 g/cm^2. These predictions are similar to Figure 3, but also include quality factors and relative biological effectiveness factors.*

The LRO/CRaTER instrument, which was launched in June 2009, measures the LET spectrum in lunar orbit as an aid in determining risks to human crews on future lunar missions. LET, often a non-linear function, is defined as the instantaneous energy

229 deposited into the local environment by a given charged particle per unit of distance. As
230 the particle's energy decreases, so does its LET. The LET spectra allow us to understand
231 the contributions to doses from different particles in the incident spectrum. Part of the
232 preparations for the mission involved estimating the LET spectrum for the anticipated
233 environment that the instrument is likely to see during the one-year operational phase of
234 the LRO mission.

235 *Townsend et al.* (2009b) prepared detailed estimates of LET spectra in the six
236 silicon detectors and two tissue-equivalent plastic segments were made using the beta-
237 version of the High Energy Transport Code for Human Exploration and Development in
238 Space (HETC-HEDS) Monte Carlo transport code. Tables of LET in each detector
239 component, for incident particle elemental species from hydrogen through iron, were
240 carried out at incident particle energies from 20 MeV/nucleon to 3 GeV/nucleon. The
241 LET values in these tables were parameterized by elemental species and energy for ease
242 in quickly and accurately estimating the LET response for any input solar or GCR
243 spectrum likely to be encountered during the lifetime of the instrument. The
244 parameterized LET values are in excellent agreement with the HETC-HEDS calculations.
245 Typical differences are on the order of a few percent.

246 Figure 5 shows a comparison between the predictions of dose rate based on the
247 *Townsend et al.* [2009b] tables and predictions using the HZETRN model. Both
248 predictions use GCR fluxes based on the *Badwhar-O'Neil* model. In the case of the
249 predictions from the HZETRN model, we consider the Lens dose behind 0.22 g/cm^2 of Al
250 shielding exposed to 1.8π ster-radian, which is appropriate for the CRaTER D1 detector.

The predictions in Figure 5 will provide useful benchmarks for comparison to CRaTER observations.

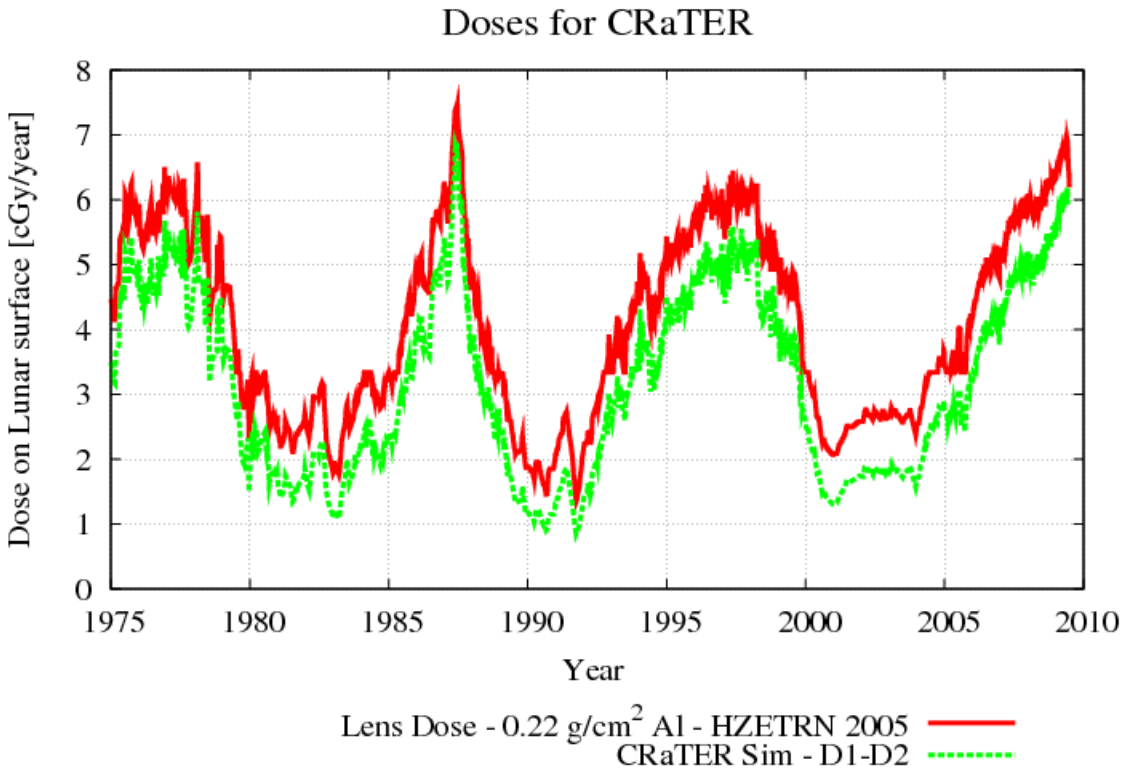

Fig. 5: Predictions of dose rates near the lunar surface for the LRO/CRaTER instrument. The red curve shows the Lens dose rate computed from HZETRN 2005 model and the Badhwar-O'Neill GCR model. The green curve uses the parameterization of LET and derived dose-rates based on the tables in Townsend et al. [2009b].

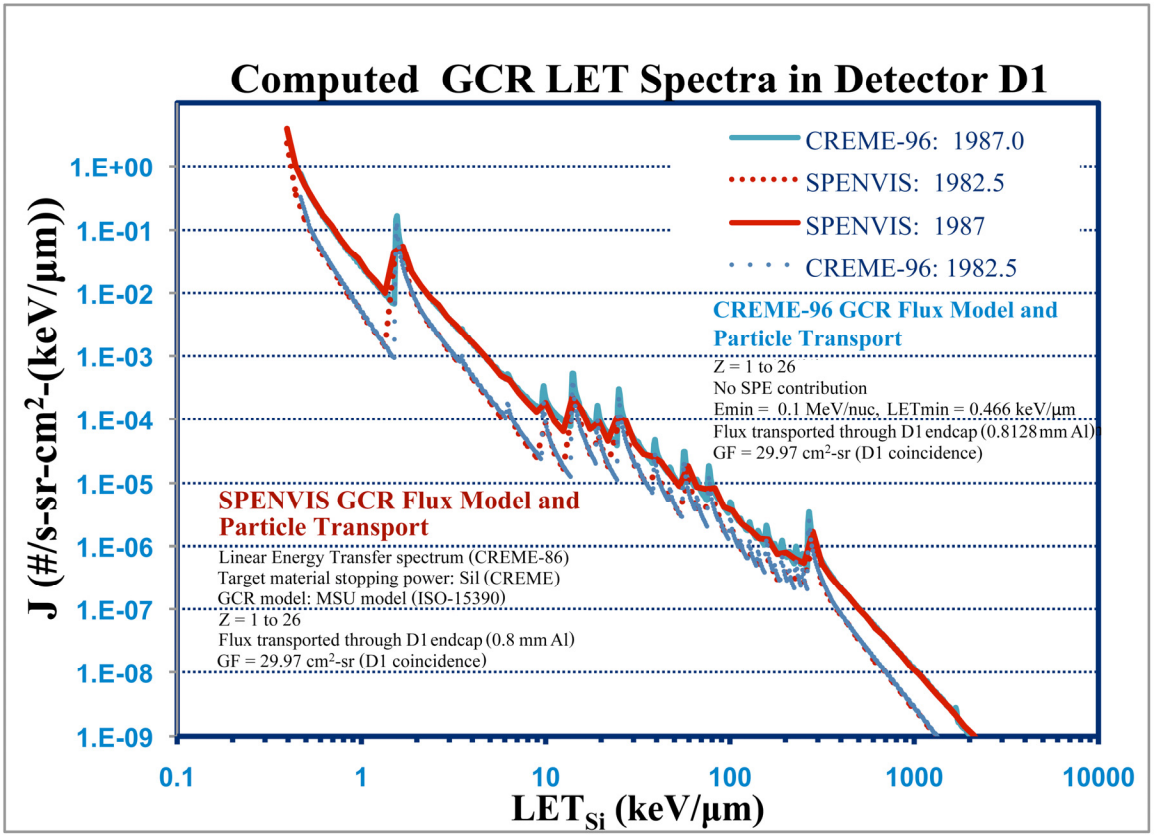

Fig. 6: Differential linear energy transfer (LET) spectra determined by the SPENVIS (http://www.spenvis.oma.be/) and CREME-96 (https://creme96.nrl.navy.mil/) models. LET energy transfer calculations allow us to differentiate the contributions to the dose in terms of species. Low LET contributions arise primarily from protons and alpha particles whereas higher LET contributions arise the heavy ions. In this case, we compute LET spectra in Si (through the D1 detector on CRaTER) using atoms with charge Z=1 to 26. The calculations were performed for a solar minimum in 1987 and a solar maximum in 1982.5.

Figure 6 shows the LET spectra determined by the SPENVIS and CREME-96 models for ions penetrating Si (through the D1 detector on CRaTER) with charge Z=1 to 26. The LET spectra show the differences between during solar minimum and solar

maximum. These predictions provide a baseline for comparison to LET spectra observed by CRaTER.

Conclusions.

We show predictions and simulations of the radiation effects induced by GCRs. The radiation environment in the extended solar minimum observed in 2009-2010 consists of highly elevated fluxes of GCRs, and accordingly, elevated dose rates. The enhanced dose rates predicted by models are the largest since 1987 and the extended solar minimum has caused an unusually long period when dose rates have been elevated. This result is not surprising considering the reduction in the total heliospheric magnetic flux observed by interplanetary spacecraft (STEREO A and B, Ulysses, ACE, and Wind). Furthermore the reduction in magnetic flux comes during a solar minimum when the heliospheric magnetic field allows better access to the inner heliosphere through gradient and curvature drifts of cosmic rays (Jokipii et al., 1977; Heber et al., 2009). In a magnetic epoch like the present when the large-scale solar magnetic fields are directed inward in the North (also in the 1960s, 1980s) we expect a more peaked time profile for positively charged GCRs. In contrast, we expect a broadened peak in the time profile of positively charged GCRs in epochs when the large-scale solar magnetic fields are directed outward in the North, as in the 1970s and 1990s. The reduction in heliospheric flux and the GCR drift patterns have caused the extended solar minimum to be both elevated in dose rate and prolonged compared to previous solar minima.

The prolonged solar minimum provides optimal conditions for the measurement of GCRs. We have used models to provide predictions for the CRaTER observations, which will be used in the coming years to test our understanding of radiation effects and

298 interactions.

299 Thus, we model the dose-rates, dose-equivalent rates and LET spectra of galactic
300 cosmic rays in the current prolonged solar minimum and make predictions for the Lunar
301 Reconnaissance Orbiter (LRO) Cosmic Ray Telescope for the Effects of Radiation
302 (CRaTER), which is now measuring GCRs in the lunar environment. Our results show
303 the weak modulation of GCRs causing the largest dose rates seen in the last 25 years over
304 the prolonged solar minimum.

305

306 Acknowledgements. Research support from the NASA LWS EMMREM project, grant
307 NNX07AC14G is gratefully acknowledged.

308

309 **References**
310

311 Badhwar, G. D. and P. M. O'Neill, An improved model of galactic cosmic radiation for
312 space exploration missions, *Proc. 22rd Int'l Cosmic Ray Conf. (Dublin)*, OG-5.2-13, 643-
313 646, 1991.

314

315 Badhwar, G. D. and P. M. O'Neill, An improved model of galactic cosmic radiation for
316 space exploration missions, *Nuclear Tracks Radiat. Mea*, 20, 403-410, 1992.

317

318 Badhwar, G. D. and P. M. O'Neill, Time lag of twenty-two year solar modulation, *Proc.*
319 *23rd Int'l Cosmic Ray Conf. (Calgary),* 3, 535-539, 1993.

320

321 Badhwar, G. D. and P. M. O'Neill, Long term modulation of galactic cosmic radiation

and its model for space exploration, *Adv. Space Res*., 14, 749-757, 1994.

Badhwar, G. D. and P. M. O'Neill, Galactic cosmic radiation model and its applications, *Adv. Space Res*., 17, 7- 17, 1996.

Beer, J. A. Bilnov, G. Bonani, H. J. Hofmann, and R. C. Finkel, Use of Be-10 in polar ice to trace the 11-year cycle of solar activity, *Nature*, 347, 164, 1990.

Burlaga, L. F., Ness, N. F., Stone, E. C., McDonald, F. B., Acuña, M. H., Lepping, R. P., and Connerney, J. E. P., Search for the heliosheath with Voyager 1 magnetic field measurements *Geophys. Res. Lett.*, 30, 2072, 2003.

Cini Castagnoli, G., et al., Evidence for enhanced 10Be deposition in Mediterranean sediments 35 Kyr BP, *Geophys. Res. Lett*., 22, 707 – 710, 1995.

Cini Castagnoli, G., G. Bonino, C. Taricco, and B. Lehman, Cosmogenic isotopes and geomagnetic signals in a Mediterranean sea sediment at 35,000 y BP, Il *Nuovo Cimento,* 21, 243– 246, 1998.

Cucinotta, F.A., Manuel, F.K., Jones, J., Izsard, G., Murray, J., Djojenegoro, and Wear, M., Space Radiation and Cataracts in Astronauts. *Radiat. Res.,* 156, 460-466 2001a.

345 Cucinotta, F. A., W. Schimmerling, J. W. Wilson, L. E. Peterson, G. D. Badhwar, P.
346 Saganti, J. F. Dicello, Space Radiation Cancer Risks and Uncertainties for Mars
347 Missions, *Radiat. Res*., 156, 682-688, 2001b.
348
349 Ferreira, S.E. and Potgieter, M.S., Long-Term Cosmic Ray Modulation in the
350 Heliosphere, *Astrophys. J.*, 603, 744–752, 2004
351
352 Florinski, V., G. P. Zank and N. V. Pogorelov, Galactic cosmic ray transport in the global
353 heliosphere, *J. Geophys. Res.,* 108, 1228, doi:10.0129/2002JA009695, 2003a.
354
355 Florinski, V., G. P. Zank and W. I. Axford, The Solar System in a dense interstellar
356 cloud: Implications for cosmic-ray fluxes at Earth and 10Be records, *Geophys. Res. Lett.,*
357 30, 2206, doi:10.1029/2003GL017566, 2003b.
358
359 Forbush, S.E. Worldwide cosmic ray variations 1937–1952. J. *Geophys. Res.,* 59, 525–
360 542, 1954.
361
362
363 Gleeson, L.J., Axford, W.I. Solar modulation of galactic cosmic rays, *Astrophys. J.,* 154,
364 1011–1026, 1968.
365
366

Ip, W.-H. and W.I. Axford, Solar modulation of galactic cosmic rays, Estimates of galactic cosmic ray spectra at low energies, *Astrophys. J.,* 149, 7-10, 1985.

Heber, B., A. Kopp, J. Gieseler, R. Muller-Mellem, H. Fichtner, K. Scherer, M. S. Potgieter, and S. E. S. Ferreira, Modulation fo galactic cosmic rays protons and electrons during an unusal solar minimum*, Astrophys. J*., 699, 1956, 2009.

Hess, V., Uber Beobachtungen der durchdringenden Stralung bei seiben Freiballonfahrten, *Phys. Zschr.,* 13, 1084-1091, 1912.

Hess, V., Uber den Ursprung der durchdringenden Stralung., *Phys. Zschr.,* 14, 610-617, 1913.

Jokipii, J. R., Levy, E. H., & Hubbard, W. B., Effects of particle drift on cosmic-ray transport. I - General properties, application to solar modulation, *Astrophys. J.*, 213, 8611977

Krimigis, S. M., Decker, R. B., Hill, M. E., Armstrong, T. P., Gloeckler, G., Hamilton, D. C., Lanzerotti, L. J., and Roelof, E. C., Evidence that Voyager-1 exited the Solar Wind at ~85 AU *Nature*, 426, 45, 2003.

Masarik, J., and J. Beer, Simulation of particle fluxes and cosmogenic nuclide production in the Earth's atmosphere, *J. Geophys. Res.,* 104, 12,099-12,111, 1999.

McComas, D. J., et al., Global Observations of the Interstellar Interaction from the Interstellar Boundary Explorer Mission, *Science,* 326, 959, doi: 10.1126/science.1180906 2009

McDonald, F. B., Cosmic-ray modulation in the heliosphere –A phenomenological study, *Space Sci. Rev.,* 83, 33–50, 1998.

McDonald, F. B., Stone, E. C., Cummings, A. C., Heikkila, B., Lal, N., and Webber, W. R., Enhancements of energetic particles near the heliospheric termination shock, *Nature,* 426, 48 – 51, 2003.

McHargue, L. R., P. E. Damon, and D. J. Donahue, Enhanced cosmic-ray production of 10Be coincident with Mono Lake and Laschamp geomagnetic excursions, *Geophys. Res. Lett.,* 22, 659–662, 1995.

McHargue, L. R., D. J. Donahue, P. E. Damon, C. P. Sonett, D. Biddulph, and G. Burr, Geomagnetic modulation of the late Pleistocene cosmic-ray flux as determined by 10Be from Blake Outer Ridge marine sediments, *Nucl. Instr. Methods Phys. Res. B*, 172, 555–561, 2000.

Millikan, R. A. and I. S. Bown, High frequency rays of Cosmic origin. I. Sounding Balloon Observations at Extreme Altitudes, *Phys. Rev*., 27, 4, 353-361, 1926

National Academy of Sciences Space Science Board, HZE Particle Effects in Manned Space Flight, National Academy of Sciences U.S.A. Washington D.C., 1973.

NASA Technical Standard, NASA-STD-3001, NASA Space Flight Human System Standar Volume 1: Crew Health, 2007.

National Academy of Sciences, NAS. National Academy of Sciences Space Science Board, Report of the Task Group on the Biological Effects of Space Radiation. Radiation Hazards to Crews on Interplanetary Mission National Academy of Sciences, Washington, D.C., 1997.

O'Neill, P. M., Galactic cosmic ray model update based on advanced composition explorer (ACE) energy spectra from 1997 to present, *Adv. Space Res*., *37*, 9, 1727, 2006.

Owens, M. J., N. A. Schwadron, N. U. Crooker, W. J. Hughes, H. E. Spence, The role of coronal mass ejections in the evolution and reversal of the coronal and heliospheric magnetic fields over the solar cycle, *Geophys. Res. Lett.,* 34*,* doi 10.1029/2006GL028795, 6104, 2007.

Owens, M. J., C. N. Arge, N. U. Crooker, N. A. Schwadron, and T. S. Horbury, Estimating total heliospheric magnetic flux from single-point *in situ* measurements, *J. Geophys. Res.,* 113*,* 12103, doi:10.1029/2008JA013677, 2008.

436

437 Parker, E.N. Passage of energetic particles through interplanetary space, *Planet. Space*

438 *Sci.,* 13, 9–49, 1965.

439

440 Potgieter, M. S., & le Roux, J. A., The simulated features of heliospheric cosmic-ray

441 modulation with a time-dependent drift model. I - General effects of the changing neutral

442 sheet over the period 1985-1990, *Astrophys. J.*, 386, 336, 1992.

443

444 Raisbeck, G. M., F. Yiou, D. Bourles, C. Lorius, J. Jouzel, and N. I. Barkov, Evidence for

445 two intervals of enhanced 10Be deposition in Antarctic ice during the last glacial period,

446 *Nature,* 326, 273-277, 1987.

447

448 Richardson, J. D., J. C. Kasper, C. Wang, J. W. Belcher, A. J. Lazarus, Cool heliosheath

449 plasma and deceleration of the upstream solar wind at the termination shock, *Nature,* 454,

450 63-66, 2008.

451

452 Saganti, P. B., F. A. Cucinotta, J. W. Wilson, T. F. Cleghorn, C. J. Zeitlin, Model

453 calculations of the particle spectrum of the galactic cosmic ray (GCR)

454 environment: Assessment with ACE/CRIS and MARIE measurements, *Radiation*

455 *Measurements,* 41, 1152 – 1157, 2006.

456

457 Scherer, K., H. Fichtner, and O. Stawicki, Shielded by the wind: The influence of the
458 interstellar medium on the environment of the Earth, *J. Atmos. Sol. Ter. Phys.,* 64*,* 795-
459 804, 2002.
460
461 Schwadron, N. A., M. Owens, N. U. Crooker, The Heliospheric Magnetic Field over the
462 Hale Cycle, *Astrophys. Space Sci. Trans.,* 4*,* 19-26, 2008.
463
464 Stone, E.C., A. C. Cummings, F. B. McDonald, B. C. Heikkila, N. Lal, W. R. Webber,
465 Voyager 1 Explores the Termination Shock Region and the Heliosheath Beyond, *Science,*
466 309, 2017, 2005.
467
468 Townsend, L., M. PourArsalan, F. A. Cucinotta, M. Y. Kim, and N. A. Schwadron,
469 Transmission of solar energetic particles and galactic cosmic rays through the Mars
470 atmosphere, *Submitted*, *Space Weather Journal*, 2009a.
471
472 Townsend, L., Y. M. Charara, N. Delauder, M. PourArsalan, J. A. Anderson, C. M.
473 Framer, H. E. Spence, N. A. Schwadron, M. J. Golightly, F. A. Cucinotta, Predictions of
474 the Linear Energy Transer Spectrum for the CRaTER Instrument During the LRO
475 Mission, Submitted, *Space Weather Journal*, 2009b.
476
477 Wagner, G., J. Masarik, J. Beer, S. Baumgartner, D. Imboden, P. W. Kubik, H.-A. Synal,
478 and M. Suter, Reconstruction of the geomagnetic field between 20 and 60 kyr BP from

479 cosmogenic radionuclides in the GRIP ice core*, Nucl. Instr. Methods Phys. Res. B*, 172,
480 597– 604, 2000.
481
482 Wilson, J. W., L. W. Townsend, W. Schimmerling, G. S. Khandelwal, F. Khan, J. E.
483 Nealy, F. A. Cucinotta, L. C. Simonsen, J. W. Norbury, Transport methods and
484 interactions for space radiations, NASA-RP1257, 1991.
485
486 T. C. Yang, K. A. George, A. Tavakoli, L. Craise, and M. Durante, Radiogenic
487 Transformation of Human Mammary Epithelial Cells *in vitro*, *Radiat. Oncol. Invest*., 3,
488 412-419, 1996.
489
490 Zank, G. P., and P. C. Frisch, Consequences of a change in the galactic environment of
491 the Sun, *Astrophys. Res.,* 518, 965-973, 1999.
492